Dielectric characterization in a broad frequency and temperature range of SrBi2Nb2O9 thin films grown on Pt electrodes

Maryline Guilloux-Viry, Jean-René Duclere, A. Rousseau, A. Perrin, D. Fasquelle, Jean-Claude Carru, Eric Cattan, Caroline Soyer, Denis Remiens, D. Fasquelle

Dielectric characterization in a broad frequency and temperature range of $SrBi_2Nb_2O_9$ thin films grown on Pt electrodes

Cite as: J. Appl. Phys. **97**, 114102 (2005); https://doi.org/10.1063/1.1904726
Submitted: 02 November 2004 • Accepted: 13 March 2005 • Published Online: 24 May 2005

M. Guilloux-Viry, J. R. Duclère, A. Rousseau, et al.

Dielectric characterization in a broad frequency and temperature range of $SrBi_2Nb_2O_9$ thin films grown on Pt electrodes

M. Guilloux-Viry,[a] J. R. Duclère,[b] A. Rousseau, and A. Perrin
Laboratoire de Chimie du Solide et Inorganique Moléculaire (LCSIM), Unité Mixte de Recherche (UMR) 6511 Centre National de la Recherche Scientifique (CNRS) Université de Rennes 1, Institut de Chimie de Rennes, Campus de Beaulieu, 35042 Rennes Cedex, France

D. Fasquelle and J. C. Carru
Laboratoire d'Etude des Matériaux et des Composants pour l'Electronique (LEMCEL), Université du Littoral Côte d'Opale, 50 rue F. Buisson, BP 717, 62228 Calais Cedex, France

E. Cattan, C. Soyer, and D. Rèmiens
Institut d'Electronique de Microélectronique et de Nanotechnologie (IEMN), Unité Mixte de Recherche (UMR)-8520, Département Opto Acousto Electronique (OAE), Matériaux et Intégration pour la Microélectronique et les Microsystèmes (MIMM), Cité Scientifique, Bâtiment P3, 59652 Villeneuve d'Ascq Cedex, France

(Received 2 November 2004; accepted 13 March 2005; published online 24 May 2005)

Ferroelectric and dielectric characteristics of two types of $SrBi_2Nb_2O_9$ thin films grown by pulsed laser deposition on Pt electrodes were determined: a randomly oriented $SrBi_2Nb_2O_9$ film (sample A), grown on a so-called polycrystalline $Pt/Ti/SiO_2/Si$ (Pt/Si) and an epitaxial $SrBi_2Nb_2O_9$ film (sample B) grown on a (110)Pt electrode epitaxially grown on $(110)SrTiO_3$. Some h00 texturation was suggested by the strong intensity of the 200 diffraction peak in sample A whereas the epitaxial sample B presents a strongly (116) preferential orientation as evidenced by x-ray diffraction and electron channeling patterns. Remanent polarization (P_r) determined from the hysteresis loops recorded on several electrodes on samples A and B was typically in the range of 5–8.5 $\mu C/cm^2$ for both samples. The Curie temperature (T_C) determined from dielectric permittivity measurements versus temperature was 705 K, for both samples, which differ, in fact, in structural characteristics but not in composition. The Curie–Weiss temperature was found lower than T_C, suggesting that the transition is of first order. The evolution of dielectric permittivity and dissipation factor was recorded versus frequency at different temperatures. At room temperature and low frequency (100 Hz), ε' is close to 150 on both films. When increasing the frequency up to 1 MHz, the ε' value decreased down to 137 for sample A and 129 for sample B. This evolution corresponds to a weak dispersion effect in relation with the high crystallization quality of the ferroelectric films. At the same time, dissipation factor $tg\delta$ increased from 1.5% to 1.8% and from 3.3% to 5.5% for samples A and B, respectively, when increasing the frequency from 100 Hz to 1 MHz. Further measurements at higher frequency were performed on the epitaxial film. As expected, dielectric permittivity decreased to about 100 when increasing the frequency to 0.5 GHz at room temperature, whereas $tg\delta$ increased up to about 9%. Decreasing the temperature down to 110 K contributes to decrease ε' from 150 at room temperature to 122 at 110 K at 1 kHz and from 100 to 87 at 0.5 GHz. Simultaneously, $tg\delta$ decreases from 8.7% to 5.6% at 0.5 GHz. © *2005 American Institute of Physics*. [DOI: 10.1063/1.1904726]

I. INTRODUCTION

Ferroelectric Aurivillius-layered compounds such as $SrBi_2Ta_2O_9$ (SBT) or $SrBi_2Nb_2O_9$ (Ref. 1) (SBN) are currently intensively investigated as thin films in view of various applications. Indeed, their fatigue-resistant properties, whatever is the nature of the electrode (metal or oxide), are of first interest for nonvolatile memories [ferroelectric random access memory (FERAM)].[2,3] Thus, several methods have been used for $SrBi_2Ta_2O_9$ or SBN thin-film deposition, such as sol-gel,[4] polymeric precursors,[5] sputtering,[6] or pulsed laser deposition (PLD).[7–9] Epitaxial growth of SBN ($a=0.551\,54$ nm, $b=0.551\,89$ nm, and $c=2.511\,24$ nm)[10] is required to study its anisotropic properties [the polarization vector lies in the (a,b) plane[11]], as well as to control the films microstructure which strongly depends on the orientation[12,13] and to avoid the grain-to-grain polarization variation in high-density integrated devices.[14,15] Several conducting oxides have been reported as potential bottom electrodes allowing an epitaxial regrowth of $SrBi_2Nb_2O_9$, such as $(La_{1-x}Sr_x)CoO_3$,[8] $YBa_2Cu_3O_{7-x}$,[6] $LaNiO_3$,[16] and $SrRuO_3$.[9] In contrast, there are only a few reports on the use of metal layers in view of SBN epitaxial growth, whereas Pt is commonly used in the case of randomly oriented films on silicon substrates. Moreover, as $SrBi_2Nb_2O_9$ presents a weak polarization fatigue,[2,3] simple metallic sublayers can be expected

[a]Author to whom correspondence should be addressed; electronic mail: maryline.guilloux@univ-rennes1.fr
[b]Present address: National Centre for Plasma Science and Technology, Dublin City University, Glasnevin, Dublin 9, Ireland

to be good candidates as electrodes for SBN. Platinum (a = 0.392 31 nm) appears as a suitable candidate for this purpose, due to its oxidization resistance, its low vapor pressure even at high temperatures, and its small misfit with both SBN and $SrTiO_3$ (a = 0.3905 nm): ~0.4% referring to $a_{SBN}\sqrt{2}/2$ or $b_{SBN}\sqrt{2}/2$, and a_{SrTiO_3}. The growth of $SrBi_2Ta_2O_9$ or $SrBi_2Nb_2O_9$ on Pt on single-crystal substrates has been reported on (100)MgO and (100)$SrTiO_3$ with (100)Pt orientation, leading to the c-axis SBN orientation.[17] We have reported on the growth of SBN on (110)Pt (Ref. 18) and (111)Pt (Ref. 19) epitaxial sublayers in view to achieve an orientation of SBN different from the c axis. This configuration is required to fit the request of a nonzero contribution of the polarization vector along the normal to the sample surface, that is achieved, for instance, for (116)SBN orientation. Otherwise, ferroelectric compounds are also of interest for applications in the microwave range, to develop, for instance, frequency tunable devices according to the variation of the dielectric constant with an applied voltage, or to elaborate small capacitive elements in microelectronic devices.[20,21] In this frame, the knowledge of the behavior of such compounds at high frequency, additionally to their low-frequency ferroelectric behavior, is of first importance.

In this paper, we report on the dielectric properties in a broad frequency range of two $SrBi_2Nb_2O_9$ thin films from which ferroelectric characteristics were previously determined at low frequency: the first one (labeled A) was deposited on a standard Pt-textured electrode on Si and the second one (labeled B) epitaxially grown on epitaxial (110)Pt grown on (110)$SrTiO_3$. Moreover, some dielectric measurements were performed at high temperature in order to record the ferroelectric/paraelectric phase transition. Dielectric permittivity and dissipation factor were also determined at low temperature in view to integrate ferroelectric films in devices with metallic as well as superconducting materials[21,22] which requires cooling of devices.

II. EXPERIMENT

A. Thin-film synthesis

~400-nm-thick $SrBi_2Nb_2O_9$ thin films were grown by pulsed laser deposition from a Bi-enriched homemade sintered target (typically 30% excess of Bi_2O_3 in weight) using a XeCl excimer laser (λ = 308 nm) operated at 2 Hz, with a fluence of about 3.5 J/cm^2 on the target. Bi enrichment is required to avoid Bi deficiency in the films deposited at high temperature, under an oxygen pressure of 0.3 mbar.[23] Two types of substrates were used: a so-called polycrystalline Pt/Ti/SiO_2/Si (Pt/Si) and a (110)Pt epitaxially grown on (110)$SrTiO_3$. In the case of polycrystalline substrates (Pt/Si), a deposition at high temperature, typically at 700 °C, leads to a predominant c orientation.[23] In order to avoid this texture, a SBN film (sample A) was deposited at 400 °C and then annealed at 750 °C in air, during 2 h. In contrast, to obtain *in situ* a SBN epitaxial film (sample B), deposition was performed at 700 °C on the (110)Pt bottom electrode. This ~200-nm-thick Pt film was deposited by dc sputtering on (110)$SrTiO_3$ single-crystal substrates from a metallic foil at 450 °C, under an Ar pressure fixed at 9 $\times 10^{-2}$ mbar and with an applied voltage of −1.5 kV.

B. Composition, structural, and microstructural analyses

Composition of the films was determined by energy dispersive spectrometry (EDS) using a Link Oxford analyzer implemented in a Jeol 6400 JSM scanning electron microscope (SEM) which gives also access to electron channeling patterns (ECP). Analysis of SBN films at low voltage (5 kV) avoids any contribution of the substrate or of the Pt sublayer in the case of SBN films typically thicker than 200 nm. The surface morphology of the films was observed with a field-effect emission scanning electron microscope (JEOL F-6301) operated at low voltage (typically 7–9 kV) in order to limit charge effects and to achieve a high resolution without the need of metallization of the samples.

Nonoriented films grown on Pt/Si were characterized by x-ray diffraction using a diffractometer equipped with a curved position-sensitive detector (INEL CPS 120, Cu $K\alpha 1$ radiation), whereas the phase analysis and growth direction of the epitaxial films were determined by θ-2θ x-ray diffraction (XRD) using an uncoupled two-axes diffractometer operated with Cu $K\alpha 1$ radiation, giving also access to mosaicity measurement (ω scans). In-plane ordering was qualitatively checked by ECP and epitaxial relationships were established by XRD φ scans recorded with a four-circle texture diffractometer (Bruker AXS D8 Discover).

C. Electrical measurements

In view of electrical characterization, the platinum layer was partially masked during the SBN deposition for bottom electrode access and 40–150-μm-diameter disk-shaped Pt top electrodes have been prepared by a lift-off process.

Hysteresis loops and fatigue tests were carried out using a standard Radiant RT6000 meter at room temperature. For hysteresis loops, the switching voltage was varied in the range of 3–20 V, which corresponds to a maximum of 500 kV/cm for SBN films with 400-nm thickness. The fatigue tests were performed at a frequency of 10^4 kHz, with an applied voltage of 7 V.

The Curie temperature was determined from dielectric constant measurements performed in the temperature range of 300–750 K at 1, 10, and 100 kHz. A homemade high-power furnace has been used to heat the films by small temperature increments of 2–10 °C. The temperature was directly measured on the samples with sensors.

For high-frequency measurements, a special cell was developed and connected to a HP4291A impedance bridge (1 MHz–1.8 GHz) or to an Anritsu 37369A vectorial networks analyzer (40 MHz–40 GHz). The dielectric permittivity ε' and loss tangent $tg\delta$ were computed from measurements in reflection (S_{11} parameter). In the low-temperature range, the films were cooled in a liquid-nitrogen cryostat.

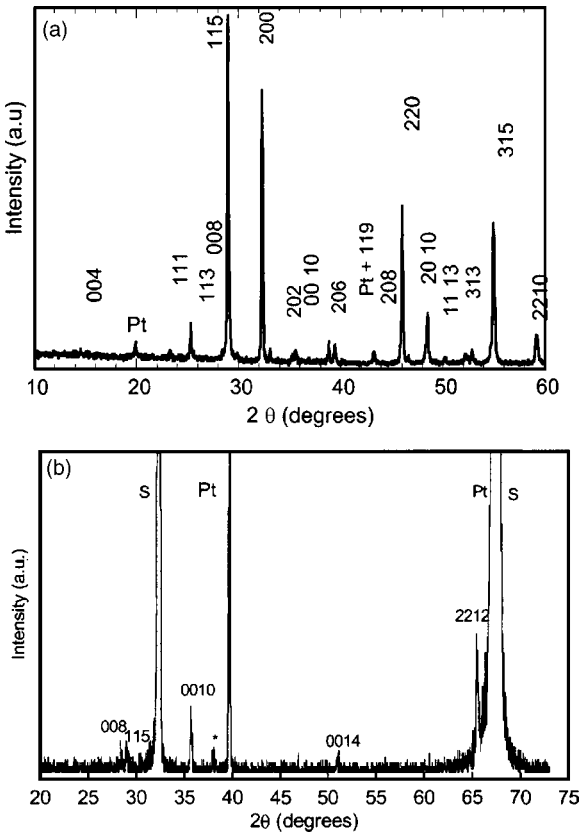

FIG. 1. X-ray diffraction patterns for $SrBi_2Nb_2O_9$ films grown (a) on Pt-coated Si (sample A) and (b) on (110)Pt epitaxially grown on (110)$SrTiO_3$ (sample B).

III. RESULTS AND DISCUSSION

A. Thin-film composition, structural, and microstructural characteristics

Composition determined by EDS was roughly the same for the two films, namely, Sr:Bi:Nb=1:2.4:2 on Pt/Si and 1:2.4:2.1 on (110)Pt. Figure 1 shows the XRD patterns of the two samples. It was evidenced that both the SBN films were single phase in spite of the excess of Bi. As expected from the low deposition temperature of 400 °C, *c*-axis preferential orientation was avoided in sample A,[23] which presents in contrast some h00 texturation suggested by the strong intensity of the 200 diffraction peak. The θ-2θ XRD pattern of sample B shows the expected preferential (116) orientation of SBN, in spite of the presence of some secondary (001) orientation, which was always observed on the films grown on (110)Pt.[18] This contrasts with the purely (116)SBN films grown on (110)$SrTiO_3$.[12] The value of 0.30° of the full width at half maximum of the rocking curve performed around the 2212 peak is the signature of the high crystalline quality of this film. The epitaxial growth of the SBN/Pt bilayer was evidenced by ECP (Fig. 2). Epitaxial relationships determined from x-ray φ scans are

$$\approx(116)_{SBN} \| (110)_{Pt} \| (110)_{STO},$$

$$[-110]_{SBN} \| [001]_{Pt} \| [001]_{STO}.$$

According to the orientation induced by the different substrates, two various microstructures were achieved, as reported on Fig. 3. Sample B presents a more homogeneous microstructure than sample A, according to the epitaxial growth along the 116 orientation leading mainly to elongated grains. Moreover some cracks can be seen in sample A, as well as in films *in situ* grown at higher temperature on Pt/Si, in contrast with sample B: growth of SBN on epitaxial Pt avoids systematically this limiting feature.

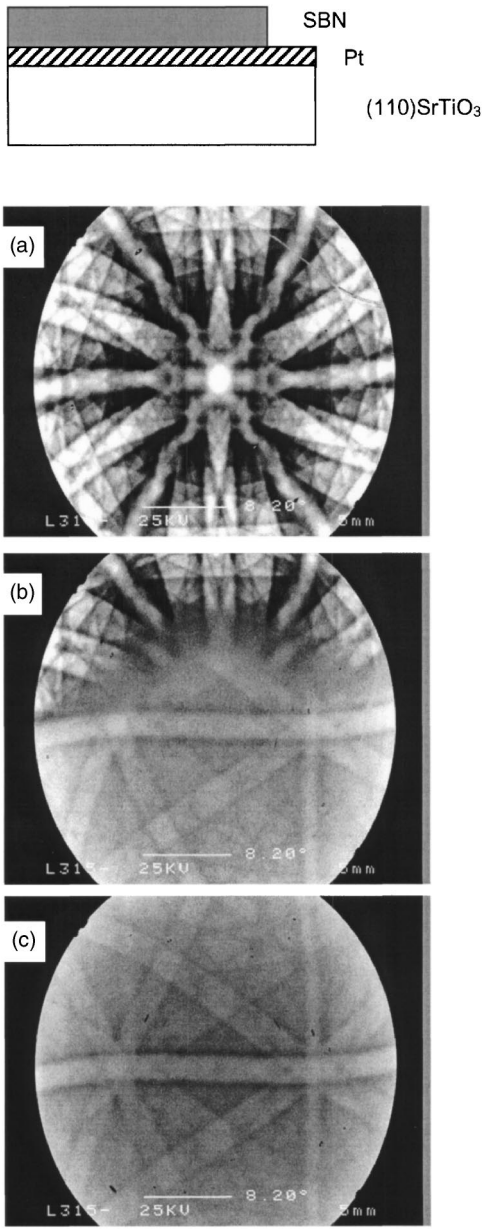

FIG. 2. Electron channeling pattern of the (110)Pt bottom electrode (a) and of the (116)$SrBi_2Nb_2O_9$ film B. (c) ECP of the median region is represented in (b). A schematic drawing of the bilayers epitaxially grown on (110)$SrTiO_3$ is given on the top of the figure.

B. Ferroelectric behavior

The hysteresis loops in Fig. 4 evidenced the ferroelectric behavior of both samples, at room temperature. Measurements were performed on several Pt top electrodes. The resulting remanent polarization (P_r) was typically in the range of 5–8.5 $\mu C/cm^2$ on samples A and B. Because of the (116) preferential orientation of sample B, a higher P_r value than

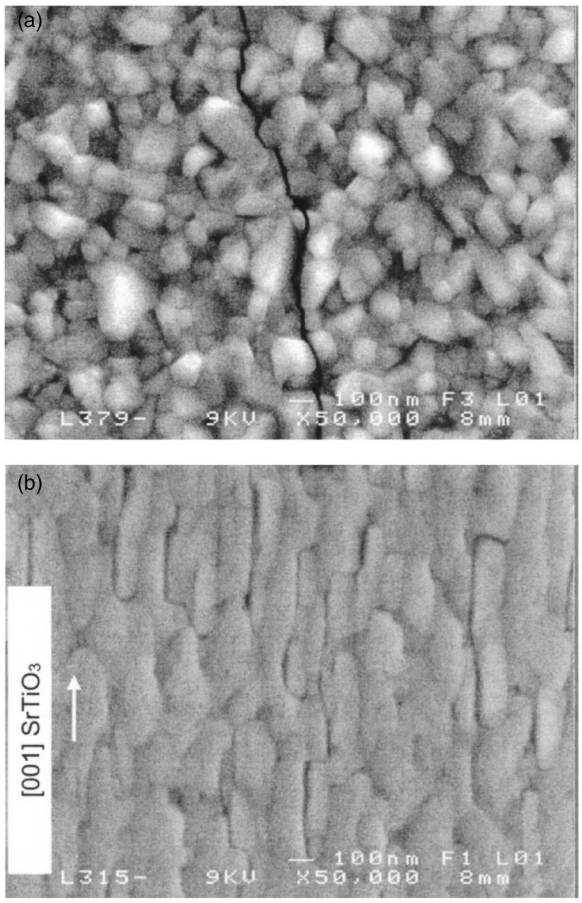

FIG. 3. Scanning electron microscopy observations of $SrBi_2Nb_2O_9$ films grown on Pt-coated Si [(a) sample A] and on (110)Pt epitaxially grown on (110)$SrTiO_3$ [(b) sample B].

the one measured on sample A could be expected. However, sample A, although polycrystalline and not epitaxially grown, presents some (200) texturation and many grains (115) oriented (Fig. 1), which contributes to increase P_r. In contrast, the presence of (001) orientation in sample B contributes to decrease P_r, which remains still lower than the best data already reported in the cases of (116) and (103)$SrBi_2Nb_2O_9$ epitaxial films deposited on (110) and (111)$SrRuO_3$ bottom electrodes, respectively.[9,24] This can explain that the values of P_r are very close on both samples A and B.

For both samples, hysteresis loops before and after fatigue tests (2×10^9 cycles) are reported on Fig. 4. The shape of the hysteresis loops is not significantly affected by fatigue effect, whereas P_r only slightly decreases. This behavior confirms the good resistance to fatigue of SBN, even on metal bottom electrode, whatever the structural characteristics.

C. Ferroelectric transition

Measurements of the dielectric permittivity ε_r were performed versus the temperature (T), during heating, at 1, 10, and 100 kHz, in order to determine the Curie point, T_C. Figure 5 displays the results obtained on both samples. The $\varepsilon_r(T)$ curves show frequency-independent maxima at 705 K, corresponding to the T_C of ferroelectric–paraelectric phase

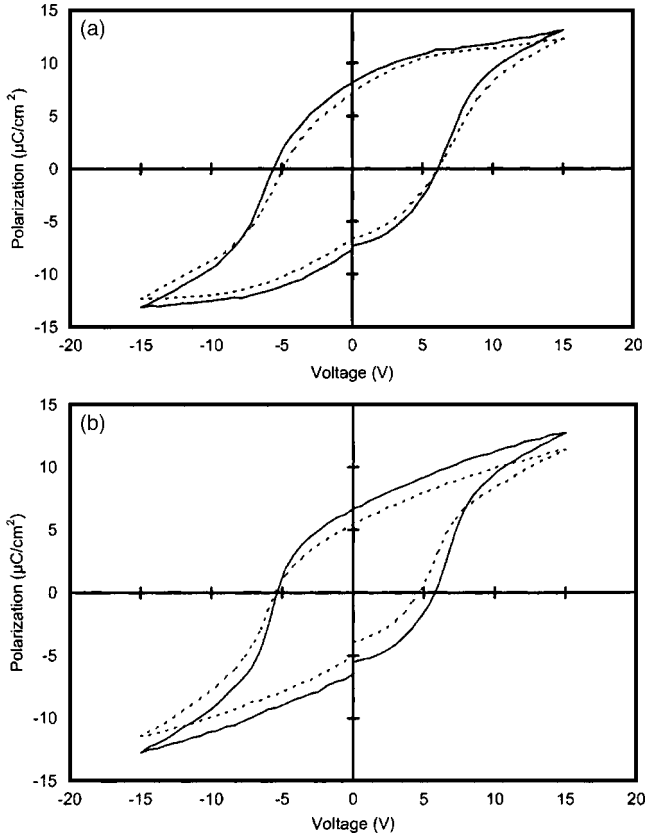

FIG. 4. Hysteresis loops recorded before (full line) and after (dotty line) fatigue tests for samples A (a) and B (b).

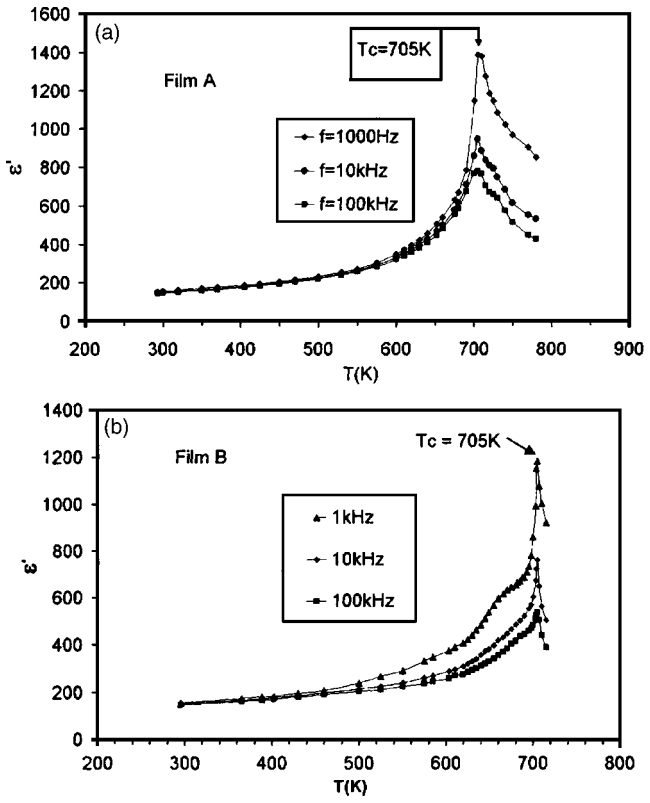

FIG. 5. Dielectric permittivity measurements vs temperature performed at 1, 10, and 100 KHz, for sample A (a) and sample B (b).

TABLE I. Dielectric characteristics of SBN thin films deposited on textured Pt on silicon (A) and epitaxially grown on (110)Pt/(110)$SrTiO_3$ (B).

Sample	Curie temperature, T_C (K)	Curie–Weiss temperature, T_θ (K)	Dielectric constant ε' at 100 kHz and 300 K	Dielectric constant ε' at 100 kHz and T_C
A	705	~620	147	778
B	705	~685	146	538

transition. The same transition temperature of 705 K was determined for both samples, which differ, in fact, in structural characteristics but not in composition. The measured T_C is slightly lower than the values of 713 and 723 K reported for bulk samples.[1,25,26] The increase of the dielectric constant from room temperature up to T_C is of the same order of magnitude than the one reported for bulk samples[1,26] in the case of the film deposited on Pt/Si, whereas it is lower for the film epitaxially grown (Table I). Below T_C the frequency dispersion of ε' is small, although higher in sample B near T_C, whereas it becomes prominent in the paraelectric region. In this region, dispersion is more prominent at low frequencies, as reported for ferroelectrics associated with ionic conductivity.[26] In fact, bulk ionic conductivity was already reported for this material.[26]

For both samples $1/\varepsilon'$ (Fig. 6) varies linearly with temperature above T_C, suggesting that the dielectric permittivity

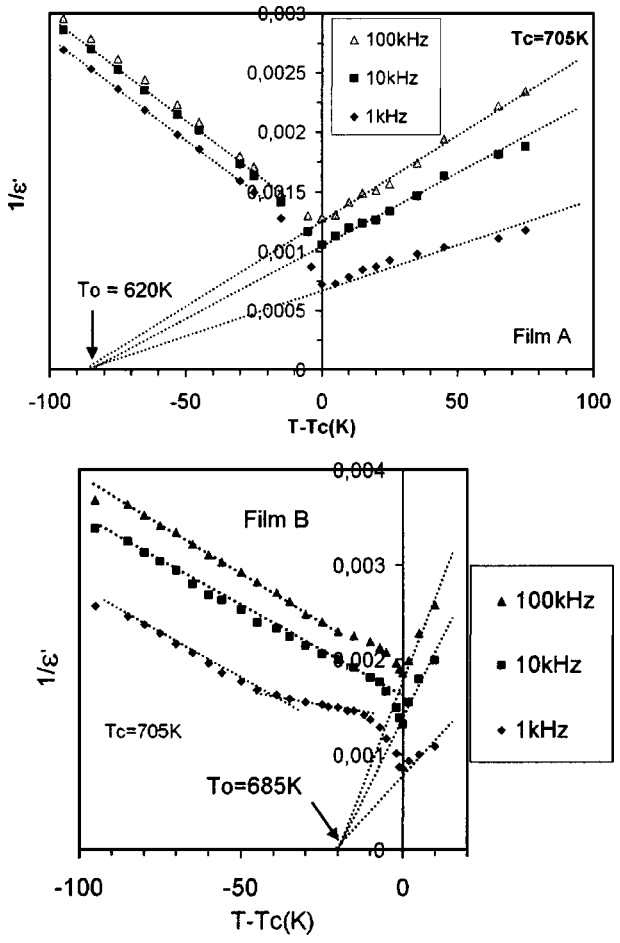

FIG. 6. Evolution of $1/\varepsilon'$ vs T-T_C for films A and B.

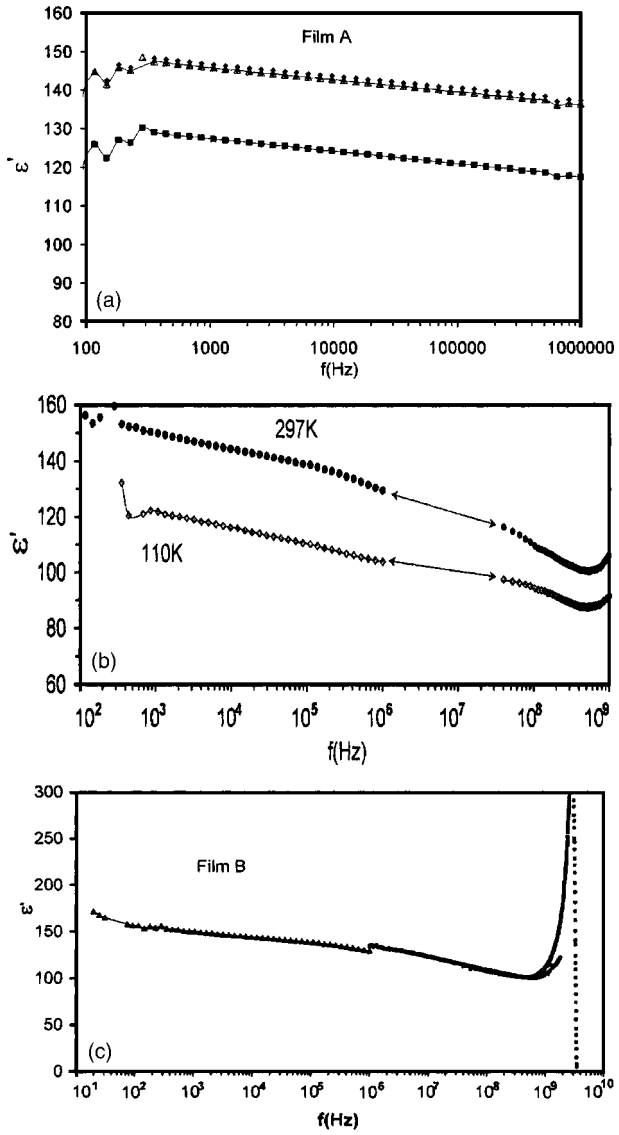

FIG. 7. Evolution of the dielectric permittivity ε' vs frequency for samples A (a) and B [(b) and (c)]. Data recorded for several electrodes are reported for sample A (a). Measurements were performed for sample B at 297 and 110 K (b).

obeys the Curie–Weiss law $[\varepsilon' = C/(T - T_\theta)]$ at all the temperatures above T_C. The Curie–Weiss temperature (T_θ) was obtained by extrapolating the linear region onto the temperature axis. T_θ was found less than T_C (Table I), suggesting that the transition is of first order. This result agrees to the conclusion of Venkataram and Varma.[26] deduced from dielectric measurements performed on bulk samples. A first-order paraferroelectric transition has been also reported recently for another Aurivillius phase ($Bi_{3.25}La_{0.75}Ti_3O_{12}$) in thin-film form.[27]

D. Evolution of dielectric permittivity and dissipation factor versus frequency at different temperatures

A first set of measurements was performed on both samples at room temperature in the frequency range of 100 Hz–1 MHz. At room temperature and low frequency (100 Hz), ε' is close to 150 for both films (Fig. 7). The data recorded for several top electrodes are reported for sample A.

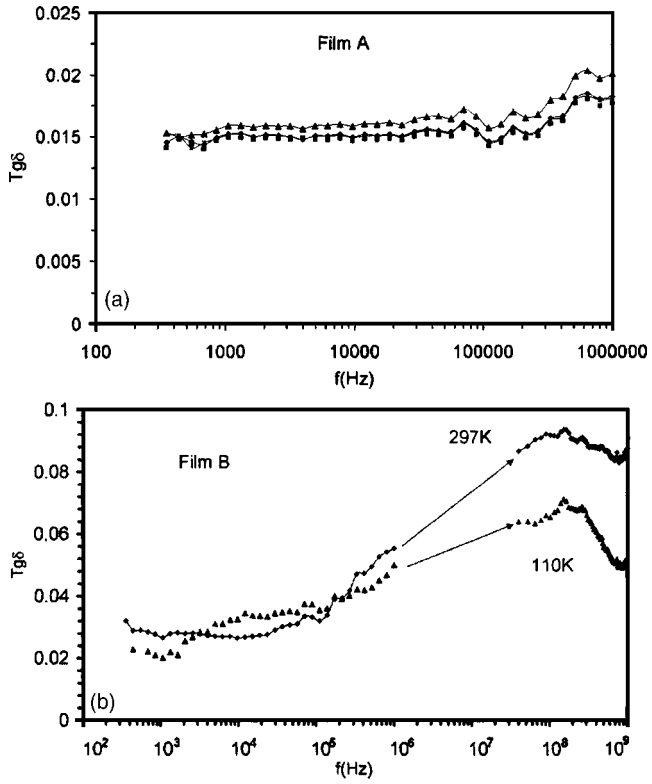

FIG. 8. Evolution of losses factor $tg\delta$ vs frequency for samples A and B. Data recorded for several electrodes are reported for sample A. Measurements were performed for sample B at 297 and 110 K.

Most values are close to 150, one is slightly lower, near 130. When increasing the frequency up to 1 MHz, ε' value decreases from 150 down to 137 for sample A and 129 for sample B (Fig. 7). This evolution corresponds to a weak dispersion effect in relation with the high crystallization quality of the ferroelectric films. In the same time, dissipation factor $tg\delta$ increases from 1.5 to 1.8 and from 3.3% to 5.5% for samples A and B, respectively, when increasing the frequency up to 1 MHz (Fig. 8). These results suggest that losses tend to be higher in the epitaxial film than in the polycrystalline one on Pt/Si. Various parameters can be responsible for this behavior such as the orientation of the ferroelectric grains, the microstructure which can affect the domains structure, and the interface between the ferroelectric film and the bottom Pt electrode. Up to now, it is not possible to distinguish between these various possible sources of losses. However, it is noteworthy that Pt bottom electrode diffuses in SBN during deposition at 700 °C, as revealed by secondary-ion-mass spectrometry[28] (SIMS), which can be responsible for losses. In the same time, the in-plane ordering arising from the epitaxial growth can make easy some ionic conductivity which can also contribute to increase losses.

A second set of measurements was performed on sample B, at higher frequency, up to 1 GHz. Three measurement setups were necessary to perform the measurements all over the frequency range from 100 Hz to 1 GHz, as described in the Experiment section. Figure 7(c) shows the good agreement between the data obtained with the various setups. As expected, dielectric permittivity decreases to about 100 when increasing the frequency to 0.5 GHz at room temperature, whereas $tg\delta$ increases up to about 9% (Figs. 7 and 8). The resonance phenomena observed above 1 GHz [Fig. 7(c)] are due to the electrical measurement circuit. Decreasing the temperature down to 110 K contributes to decrease ε' from 150 at room temperature to 122 at 110 K at 1 kHz, and from 100 to 87 at 0.5 GHz. Simultaneously, $tg\delta$ decreases from 8.6 to 5.7% at 0.5 GHz (before the resonance). The comparison of measurements performed at room temperature and at low temperature gives access to an evaluation of the intrinsic contribution to ε'. Indeed, at 1 MHz, for example, the value of ε' is 130 at room temperature and 105 at 110 K, which suggests that the extrinsic contribution is of about 25% at middle frequency and that the intrinsic value of ε' is about 100. In this case extrinsic contribution can be due to domain-walls motion and to some ionic conductivity mainly associated with oxygen vacancies. We can notice that dispersion was also reduced by decreasing temperature. The evolution of ε' and $tg\delta$ with frequency can suggest a relaxation mechanism. However, in this frequency range this phenomenon should be thermally activated. In contrast the extrema of the curves are placed at the same frequency at 297 and 110 K, so this phenomenon is not thermally activated. Measurements at higher frequencies up to 10 GHz are needed to see if ε' and $\varepsilon''=\varepsilon'$. $tg\delta$ follows the empirical Curie–von Schweidler law.[29]

IV. CONCLUSION

The dielectric behavior of $SrBi_2Nb_2O_9$ thin films grown by pulsed laser deposition either on textured Pt/Si or on epitaxial (110)Pt/(110)$SrTiO_3$ bottom electrodes was investigated. Quite similar behavior was observed for the two samples, suggesting that the difference of orientation and microstructure does not strongly affect it. However, some differences have to be pointed out such as the presence of cracks in the film on Pt/Si leading to many short circuits, and indeed it has been impossible to perform electrical measurements on several electrodes. To avoid cracks in SBN films on Pt-coated silicon some specific processes such as rapid thermal annealing are generally proposed in place of standard heating treatments. In contrast only a small percentage of electrodes tested was in short circuit (typically 5%–10%) in the case of (110)Pt/(110)$SrTiO_3$. Moreover the main interest of epitaxial films consists of the homogeneity of the behavior from one grain to another one in view of miniaturization of devices, as evidenced on similar SBN films epitaxially grown on (110)Pt on (110)$SrTiO_3$.[30]

SBN thin films can be potential candidates for applications in devices operating at high frequency, taking into account the weak dispersion observed from 500 Hz to 1 GHz in both types of samples: either for high dielectric permittivity gate insulator or for tunable devices. However, the quite high dissipation factor constitutes a limitation for some applications and has to be considered. Further investigations on SBN films grown on other substrates compatible with microwaves applications are required to determine if it is possible to decrease the dissipation factor. For example, complementary studies on *c*-axis SBN films deposited on bare (100)MgO or $LaAlO_3$ substrates will provide additional data

in this way. In fact, in spite of quite high losses associated up to now with this material we have to point out that a tunable resonator operating near 10 GHz was realized with *c*-axis SBN films epitaxially grown on a (100)MgO substrate.[31]

ACKNOWLEDGMENTS

This work was supported by CNRS under "Materials Program" and by Région Bretagne under Contract CACET No. A2CA33. SEM (including EDS and ECP) was performed at CMEBA at University of Rennes 1. The authors from LCSIM warmly thank L. Burel for technical assistance.

[1]E. C. Subbarao, J. Phys. Chem. Solids **23**, 665 (1962).
[2]C. A-Paz de Araujo, J. D. Cuchlaro, L. D. McMillan, M. C. Scott, and J. F. Scott, Nature (London) **374**, 627 (1995).
[3]J. F. Scott, F. M. Ross, C. A-Paz de Araujo, M. C. Scott, and M. Huffman, MRS Bull. **21**, 33 (1996).
[4]J. H. Yi, P. Thomas, M. Manier, J. P. Mercurio, I. Jauberteau, and R. Guinebretière, J. Sol-Gel Sci. Technol. **13**, 885 (1998).
[5]S. M. Zanetti, E. R. Leite, E. Longo, and J. A. Varela, J. Mater. Res. **13**, 2392 (1998).
[6]Ch. Schwan, P. Hailbach, G. Jacob, J. C. Martinez, and H. Adrian, J. Appl. Phys. **86**, 960 (1999).
[7]H.-M. Yang, J.-S. Luo, and W.-T. Lin, J. Mater. Res. **12**, 1145 (1997).
[8]A. Pignolet, S. Welke, C. Curran, S. Senz, and D. Hesse, J. Korean Phys. Soc. **32**, 1476 (1998).
[9]J. Lettieri, M. A. Zurbuchen, Y. Jia, D. G. Schlom, S. K. Streiffer, and M. E. Hawley, Appl. Phys. Lett. **77**, 3090 (2000).
[10]D. Ismunandar, B. J. Kennedy, M. Gunawan, and P. Marsongkohadi, J. Solid State Chem. **126**, 135 (1996).
[11]Y. Shimakawa, Y. Kubo, Y. Nakagawa, S. Goto, T. Kamiyama, H. Asano, and F. Izumi, Phys. Rev. B **61**, 6559 (2000).
[12]J. R. Duclère, M. Guilloux-Viry, and A. Perrin, J. Appl. Crystallogr. **36**, 96 (2003).
[13]A. Rousseau, J.-R. Duclère, M. Guilloux-Viry, V. Bouquet, and A. Perrin, Ann. Phys. **13**, 55 (2004).
[14]A. Gruverman, Appl. Phys. Lett. **75**, 2839 (2000).
[15]G. Asayama *et al.*, Appl. Phys. Lett. **80**, 2371 (2002).
[16]A. Pignolet, C. Schäfer, K. M. Satyalakshmi, C. Harnagea, D. Hesse, and U. Gösele, Appl. Phys. A: Mater. Sci. Process. **70**, 283 (2000).
[17]S. B. Desu, D. P. Vijay, X. Zhang, and B. P. He, Appl. Phys. Lett. **69**, 1719 (1996).
[18]J. R. Duclère, M. Guilloux-Viry, A. Perrin, E. Cattan, C. Soyer, and D. Rèmiens, Appl. Phys. Lett. **81**, 2067 (2002).
[19]J.-R. Duclère, M. Guilloux-Viry, V. Bouquet, A. Perrin, E. Cattan, C. Soyer, and D. Rèmiens, Appl. Phys. Lett. **83**, 5500 (2003).
[20]S. S. Gevorgian, IEEE Trans. Microwave Theory Tech. **49**, 2117 (2001).
[21]M. J. Lancaster, J. Powell, and A. Porch, Supercond. Sci. Technol. **11**, 1323 (1998).
[22]Y. A. Boikov, Z. G. Ivanov, E. Olsson, and T. Claeson, Physica C **282–287**, 111 (1997).
[23]J. R. Duclère *et al.*, Int. J. Inorg. Mater. **3**, 1133 (2001).
[24]J. Lettieri, M.-A. Zurbuchen, Y. Jia, D.-G. Schlom, S.-K. Streiffer, and M.-E. Hawley, Appl. Phys. Lett. **76**, 2937 (2000).
[25]Y. Shimakawa, Y. Kubo, Y. Tauchi, T. Kamiyama, H. Asano, and F. Izumi, Appl. Phys. Lett. **77**, 2749 (2000).
[26]B. H. Venkataraman and K. B. R. Varma, J. Phys. Chem. Solids **64**, 2105 (2003).
[27]D. Wu, A. Li, and N. Ming, Appl. Phys. Lett. **84**, 4505 (2004).
[28]J. R. Duclère *et al.*, J. Phys. IV **11**, 133 (2001).
[29]A. K. Jonscher, *Dielectric Relaxation in Solids* (Chelsea Dielectrics, London, 1983).
[30]B. Gautier, J.-R. Duclère, and M. Guilloux-Viry, Appl. Surf. Sci. **217**, 108 (2003).
[31]A. Gensbittel, A. F. Dégardin, A. J. Kreisler, M. Guilloux-Viry, A. Perrin, and P. Crozat, Ferroelectrics **288**, 103 (2003).